The Stratospheric Terahertz Observatory (STO):
An LDB Experiment to Investigate the Life Cycle of the Interstellar Medium

Science Investigation

1 Executive Summary

The structure of the interstellar medium, the life cycle of interstellar clouds, and their relationship with star formation are processes crucial to deciphering the internal evolution of galaxies. Rapid, high resolution spectral line imaging of key gas tracers not accessible from the ground are needed to fill in major missing pieces of Galactic structure and witness the formation and dissipation of interstellar clouds. The Stratospheric Terahertz Observatory (STO), a balloon-borne 0.8-meter telescope with an 8-beam far-infrared heterodyne spectrometer, will address these issues and significantly advance NASA's Strategic Sub-goal 3D (discovering the origin, structure, evolution and destiny of the universe) and research objectives 3D.2 (the evolution of galaxies) and 3D.3 (star formation).

In its first long duration flight, STO will survey part of the Galactic plane in [C II] line emission at 158 μm, the brightest spectral line in the Galaxy; and [N II] line emission at 205 μm, a tracer of the star formation rate. At $\sim 1'$ angular resolution and $<$1 km/s velocity resolution, **STO will detect every interstellar cloud with $A_V \geq 0.4$ in the surveyed region**, and, through excitation and kinematic diagnostics provided by [C II] and [N II] line emission, **will illustrate how atomic and molecular clouds are formed and dispersed in the Galaxy**. STO will make 3-dimensional maps of the structure, dynamics, turbulence, energy balance, and pressure of the Milky Way's Interstellar Medium (ISM), as well as the star formation rate. While this proposal focuses on the science from the first long duration ($\sim$10-14 day) flight, we briefly discuss subsequent flights since the possibility of additional flights with new instrument configurations is one of the core strengths of a balloon project. Subsequent flights will target [C II] and [N II] in the Galactic center and the outer Galaxy, and selected mapping of denser regions with infrared [O I], [N II] and HD lines. This summary section briefly describes science goals, mission approach, and complementarity with other missions; subsequent sections 2-5 go into more detail on each topic.

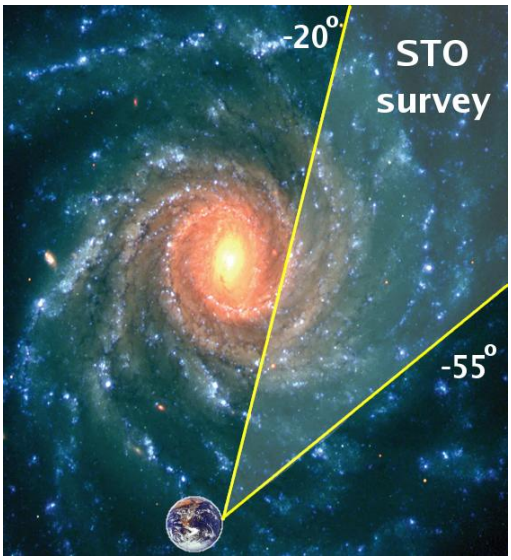

Figure 1: Overview of the region to be surveyed by STO. This 35° longitudinal swath of the Galactic Plane reveals major components of the Milky Way ISM, such as the molecular ring, the Scutum-Crux spiral arm, and the interarm region.

1.1 Summary: Science Goals and Objectives

STO will provide a comprehensive understanding of the inner workings of our Galaxy by exploring the connection between star formation and the life cycle of interstellar clouds. We will study the formation of molecular clouds from diffuse atomic gas, the feedback of high mass star formation on the lives of atomic and molecular clouds, and the effect of these processes upon the global structure and evolution of the Galaxy. The detailed understanding of star formation and evolution of stars and gas in the Galaxy is directly relevant to star formation in other galaxies. The nature of the feedback mechanism of massive star formation with its interstellar environment is pivotal to the evolution of galaxies. STO thus addresses NASA's goals and research objectives on galaxy evolution and star formation. **In its first flight, STO addresses the high priority goals:**

1. **Determine the life cycle of Galactic interstellar gas.**
2. **Study the creation and disruption of star-**

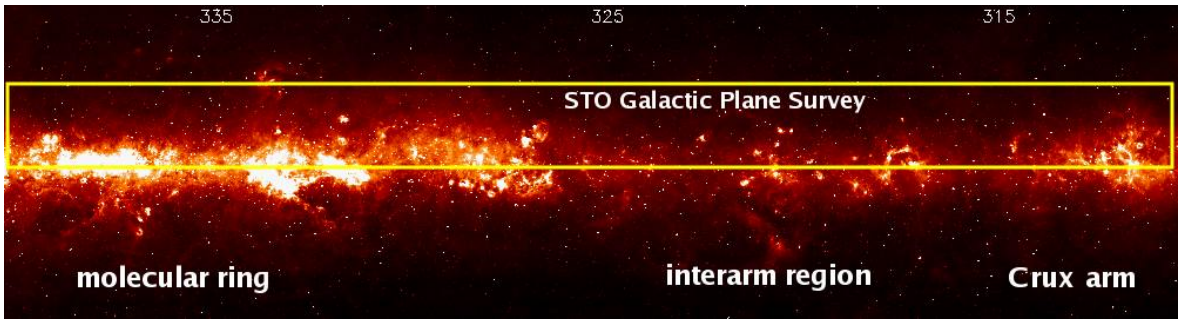

Figure 2: Midcourse Space Experiment (MSX) 8.3 μm map of the Galactic Plane from the Molecular Ring through the Scutum-Crux Spiral Arm ($-20^\circ > l > -55^\circ$). The yellow rectangle highlights the region to be explored by STO on its first long duration flight.

forming clouds in the Galaxy.

3. **Determine the parameters that affect the star formation rate in a galaxy.**
4. **Provide templates for star formation and stellar/interstellar feedback in other galaxies.**

1.2 Summary: Mission Approach

STO will utilize two heterodyne receiver arrays to produce a total of eight $\sim 1'$ pixels in the focal plane, each with 1024 spectral channels. In the first long duration (10-14 day) flight STO will map a 35 square degree area including the Galactic molecular ring (Figures 1 & 2) as well as two deeper, 1/2 square degree maps in arm and interarm regions. STO has the sensitivity to detect and the ability to resolve spectrally and spatially all Giant Molecular Clouds (GMCs), all significant H II regions, and all cold neutral medium (CNM) atomic clouds with $A_V \geq 0.4$ mag in the surveyed region.

The STO heterodyne receivers provide sub-km/s velocity discrimination and sufficient bandwidth to detect and resolve line emission from every Galactic cloud in the surveyed region. The data products envisioned include:

1. A high fidelity database of spatially and velocity resolved far-infrared [C II] 158 μm and [N II] 205 μm fine-structure line emission in the Galaxy.
2. A combination of STO's data products with existing line and continuum surveys to characterize the structure and dynamics of interstellar clouds and their relation to star formation.

The data are produced in large scale (Galactic Plane Survey) and selective (Deep Survey) modes:

- **GPS: Galactic Plane Survey**: $-20^\circ > l > -55^\circ$; $0^\circ < b < 1^\circ$
- **DS: Deep Survey** of arm and interarm regions: $l \sim -50^\circ$ and $l \sim -40^\circ$; $\sim 0.5 - 0.7^\circ$ in b

STO's potential for additional flights provides the ability to more fully map the Galaxy in the [C II] and [N II] lines and to change receivers to include other important interstellar lines such as [N II] 122 μm, [O I] 63 & 145 μm, and HD 112 μm.

1.3 Summary: Complementarity with Other Missions and Existing Data

STO is timely. STO will provide the best corresponding interstellar cloud survey to the GLIMPSE and MIPSGAL Spitzer Legacy programs and contemporary H I and CO line surveys. STO will enhance the interpretation of these data sets by completing the observational links required to trace the cloud life cycle. In addition, STO complements other [C II] and [N II] observations taken on the Cosmic Background Explorer (COBE) and the Balloon-borne Infrared Carbon Explorer (BICE) in having much greater spatial and spectral resolution. Using Galactic rotation to place the clouds along the line of sight, STO's high spectral resolution enables 3 dimensional maps of Galactic interstellar matter, from which many physical parameters in the Galaxy (e.g., pressure and star formation rate) can be extracted.

STO also complements the capabilities of heterodyne receivers on contemporary far-IR platforms. The Herschel Space Observatory (Science phase:2009-2013) and the Stratospheric Observatory for Infrared Astronomy (SOFIA, 2009+) will have the capability to observe both [C II] and [N II] using the same high spectral resolution heterodyne techniques used on STO. However, due to their much larger apertures each facility will map only a few percent of the area of STO's first survey during their

lifetimes.

2 Overview

2.1 *Background and Objectives*

Via spatially and spectroscopically resolved [C II] and [N II] line emission, STO probes uniquely the pivotal formative and disruptive stages in the life cycles of interstellar clouds. It reveals new insight into the relationship between interstellar clouds and the stars that form from them, a central component of galactic evolution.

Neutral interstellar gas is the dominant mass component of the ISM, and tends to exist as two phases in rough thermal pressure equilibrium: a diffuse warm neutral medium (WNM) with hydrogen densities at the solar circle of $n \sim 0.3$ cm^{-3} and T$\sim$8000 K, and a denser, colder CNM with $n \sim$40 cm^{-3} and T$\sim$70 K (Kulkarni & Heiles, 1987; Wolfire et al., 2003). Turbulence provides a broader spectrum of conditions (Mac Low et al., 2005; Gazol et al., 2005), but thermal balance drives neutral gas toward these phases. With sufficient shielding column, $N > 10^{20} - 10^{21}$ cm^{-2} of hydrogen nuclei, the CNM clouds begin to harbor molecular interiors. Above $N \sim 10^{22}$ cm^{-2} they become fully-molecular, gravitationally bound and stars may form in their interiors (McKee, 1989). The largest condensations take the form of GMCs with large masses $10^5 - 10^6$ M$_\odot$ and are responsible for most of the star formation in the Galaxy. These ISM components are shown schematically in Figure 3.

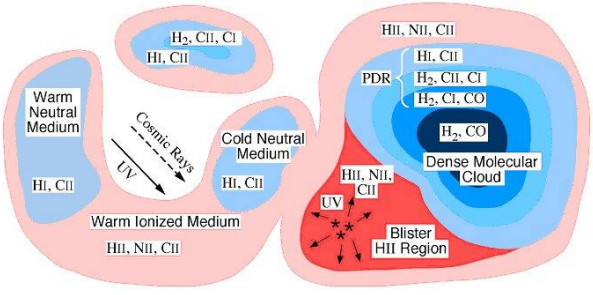

Figure 3: Schematic representation of ISM components. STO detects and maps in the Galaxy the higher column density CNM component, the H_2/C^+ component, the photodissociation region (PDR) surfaces of molecular clouds, the H II component and (with H I) the WNM/CNM ratio.

WNM is converted into CNM clouds via thermal instability either if the ultraviolet radiation field (heating) diminishes (Parravano et al., 2003) or if the pressure increases because of the passage of a (e.g., supernova) shock wave (McKee & Ostriker, 1977). GMCs presumably form from a large assemblage of CNM clouds; the leading theoretical models invoke gravitational instabilities in huge regions 0.5-1 kpc in size along spiral arms (Ostriker & Kim, 2004) although this assemblage process has never been directly observed and other mechanisms have been invoked such as the convergence of flows in a turbulent medium (Hennebelle & Pérault, 2000; Heitsch et al., 2006).

The ultraviolet radiation from massive stars not only heats the CNM and WNM and determines the relative portions of these phases, but it also ionizes gas and heats it to 10^4 K, producing H II regions. [N II] line emission provides an extinction-free measure of ionizing radiation from young, massive stars (a direct measure of star formation rates), and [C II] and [N II] together measure the disruptive impact of UV radiation on the surfaces of neighboring clouds; a key part of the stellar/interstellar feedback that governs galactic evolution. GMCs are primarily destroyed by the ultraviolet radiation from OB stars which form inside and lie relatively close to their natal GMCs (Williams & McKee, 1997). This stellar feedback likely determines the fraction of cloud gas which is converted to stars. CNM clouds are destroyed by the interstellar UV field produced by the global (many hundreds of pc) OB stellar population. If global star formation rates are high, the interstellar field is high, thereby lowering the CNM population by converting them to ionized or WNM gas. This conversion then lowers the rate of GMC formation, and thus the global star formation rate. These stellar feedback effects could regulate star formation rates in galaxies.

Joined with other surveys, STO will:

1. Map as a function of Galactic position the size and mass distribution and internal velocity dispersion of atomic, molecular and ionized clouds in the Galaxy.
2. Construct the first barometric map of the Galaxy, the first map of the gas heating rate, and a more sensitive and detailed map of the star formation rate.
3. Reveal clouds clustering and forming in spiral arms and supershells, and follow the growth of clouds to sufficient column densities to shield molecules and to become gravitationally bound
4. Measure the destruction rate of clouds via the

conversion to warm ($\sim 10^4$ K), diffuse neutral and ionized gas.

5. Observe the formation and destruction of clouds throughout the Galaxy, test turbulent theories of these processes, and directly observe the feedback effects caused by supernovae and the ultraviolet radiation from young massive stars.
6. In conjunction with H I surveys, map the mass ratio of CNM to WNM, so that we may correlate this ratio with thermal pressure, ultraviolet radiation field, and star formation rate.
7. Probe the relation between the mass surface density (on kpc scales) and the star formation rate, so that we may be able to understand the empirical Schmidt Law, which relates star formation rates to gas mass surface density.

2.2 *Overview of STO Capability*

STO achieves 3σ intensity limits of 2.0×10^{-5} (t/1 sec)$^{-1/2}$ and 8.0×10^{-6} (t/1 sec)$^{-1/2}$ erg s^{-1} cm^{-2} sr^{-1} in the [C II] and [N II] lines. With this sensitivity, STO can detect the GMCs, CNM clouds, and H II regions discussed above. The CNM clouds typically have sizes r$\sim$3 pc and subtend $> 1'$ of angle at a distance of 8.5 kpc, filling the STO beam. These CNM clouds will therefore be both spatially and spectrally resolved. STO will resolve in [C II] the surfaces of all GMCs illuminated by the local (or brighter) interstellar radiation field and the [C II] and [N II] emission from H II regions with Emission Measure (EM) > 50 cm^{-6} pc. [C II] originates in both neutral and ionized gas, whereas [N II] arises solely from ionized gas. STO [N II] observations will provide the most sensitive and detailed maps of star formation rates in the Galaxy, and are crucial for separating the ionized and neutral components of [C II] emission.

The main features of STO surveying modes are:

- High spatial resolution, $\sim$1 arcmin (3 pc at $d =$ 10 kpc).
- Very high spectral resolution, $<$1 km/s.
- High dynamic range: 10^4 spatially and 10^3 spectrally
- More than 10^5 spatial pixels
- High sensitivity: 10^4 times better than FIRAS/COBE when convolved to the same resolution. STO will catalogue all neutral clouds with columns $N > 5 \times 10^{20}$ cm^{-2} and all ionized clouds with EM > 50 cm^{-6} pc

Figure 4 shows the STO sensitivity to various cloud components, and Figure 5 shows a simulation of [C II], CO and H I spectra along a line of sight through the Galaxy. Observed CO and H I spectra (top) and simulated [C II] spectrum are provided for 10s integration (middle) and 200s integration (bottom). The simulations indicate that three distant CNM clouds of columns (left to right) of 3, 5, and 7 $\times 10^{20}$ cm^{-2} are detectable. The H I has a considerable WNM component. The blue peaks shown in the figure are surfaces of molecular clouds. Toward illuminated cloud surfaces, particularly in deep surveys, STO will detect the [^{13}CII] fine structure line, which exhibits three hyperfine components at shifts of +11, +63, and -65 km/s relative to the [^{12}CII] line. Here, measurements of the [^{13}CII]/ [^{12}CII] line ratio will probe the [^{12}CII] optical depth and the ^{13}C/^{12}C abundance ratio (Boreiko & Betz 1996).

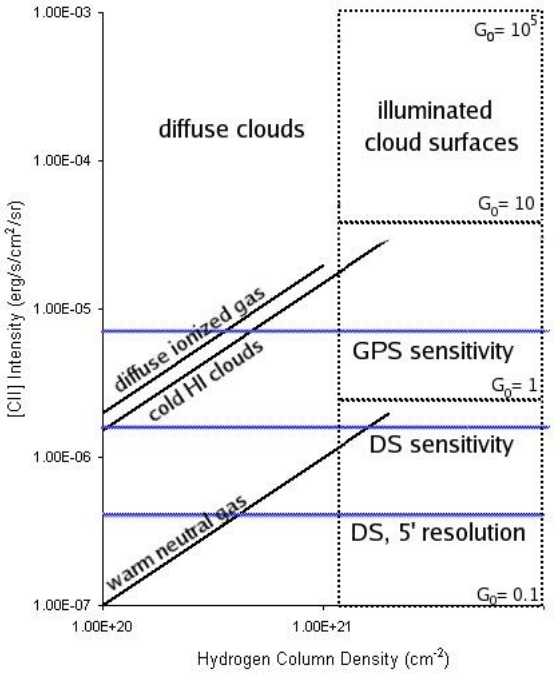

Figure 4: Comparison of STO's sensitivity with [C II] integrated intensity for diffuse interstellar components which constitute the building blocks for molecular clouds (diagonal lines), and UV-irradiated molecular cloud surfaces (dotted boxes). The external radiation fields are quantified in units of the local interstellar radiation field G_0. The corresponding sensitivities (3σ rms noise) of STO's two survey modes (see section 1.2 for definitions) are indicated by solid blue lines.

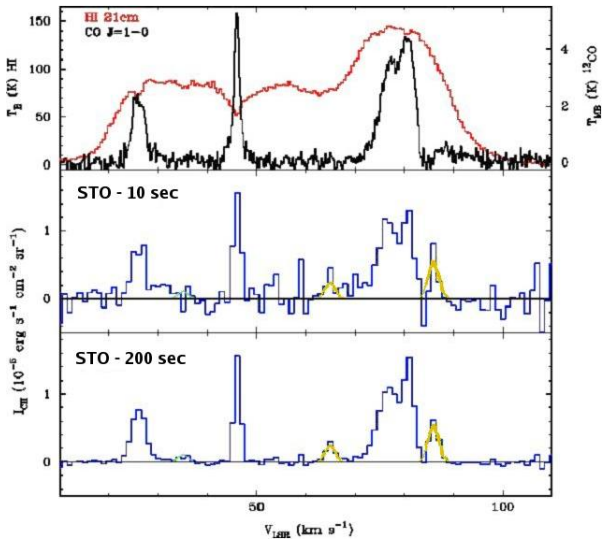

Figure 5: Observed CO and H I spectra (top) and simulated [C II] spectra for 10 seconds (middle) and 200 seconds (bottom) integration. The green curves indicate three distant CNM clouds.

3 Specific Science Goals and Objectives

Goal 1: Anatomy of Interstellar Gas

STO's unique blend of sensitivity, angular resolution and spectral resolving power allows it to map and diagnose *all components of the warm and cold interstellar medium*. STO will survey spiral arm, interarm regions and a large portion of the molecular ring, where much of the star formation occurs in the Galaxy. Galactic rotation allows velocity separation of the clouds along the line of sight. Therefore, *STO will provide an unprecedented 3D global map of the distribution of clouds of ionized gas, atomic gas, and molecular clouds (via their dense atomic surfaces) as a function of Galactocentric radius (R) and height (z) in the Galaxy*. We can compute the density of clouds (i.e., the number of clouds per kpc^3) and their size distribution as functions of R and z, and see how clouds are clumped together in spiral arms or supershells. In regions of cloud clustering, the superb velocity resolution of STO will measure the random motions of clouds, and diagnose *large scale turbulence*.

COBE FIRAS observations show that the ionized component of the ISM radiates strongly in both [C II] 158 μm and [N II] 205 μm (Wright et al., 1991). To distinguish the origin(s) of [C II] emission, velocity-resolved measurements of the small scale distribution of the ionized gas must be made in [N II] and compared to the [C II] distribution. *STO will conclusively determine the origin of the [C II] emission from various regions in the Galaxy*, and will enable the portion of the [C II] emission coming from the CNM neutral gas to be unambiguously determined.

If the CNM clouds are seen in H I, which determines their column and mass, the ratio of CNM [C II] to H I intensity provides a measure of the [C II] emissivity per H atom which rises monotonically with gas density and thermal gas pressure. *The STO survey over a large portion of the Galactic Plane thereby enables the construction of the first barometric maps of the Galactic disk*, determining the ambient thermal pressure in different environments (e.g., the spiral arms versus interarm regions, turbulent versus quiescent regions). The STO team's theoretical models are vital to determining the density, temperatures, and thermal pressures in the clouds. These pressure maps and the maps of cloud distributions and properties can be correlated with star formation rates to understand stellar/interstellar feedback mechanisms.

Where extended emission is seen in H I with no [C II] counterpart, we can attribute the H I emission to extended low density gas – either WNM or thermally unstable gas with densities below that of CNM (Figure 5). To achieve the required sensitivity, we will smooth the data to larger ($\sim$10 km/s) velocity and spatial ($\sim$ 10′) bins. In this way, STO can map the CNM/WNM mass fraction in the Galaxy, and determine how much of the neutral gas is in clouds rather than in warm or unstable components. This ratio can be correlated to the thermal pressure, to the ultraviolet radiation field, and to the star formation rate to probe the stellar feedback processes that regulate star formation.

In addition, the [C II] line dominates the cooling of CNM clouds. Therefore, we directly obtain the gas heating rate of clouds as a function of radius throughout the Galaxy. Besides the fundamental interest in tracing the energy flow in the Galaxy, the observations also can test our theoretical hypothesis that the heating is provided by the grain photoelectric heating mechanism in diffuse clouds. This hypothesis has been tested (positively) in denser clouds illuminated by stronger fields, but it is not yet certain that in weak UV fields other mechanisms may be important. The test involves correlating the heating with the observed incident radiation field and the gas density in a sample of clouds.

Goal 2: Formation & Destruction of Clouds

The formation of interstellar clouds is a prerequisite for star formation, yet the process has not yet been directly observed! **STO is designed with the unique combination of sensitivity and resolution needed to observe cold atomic clouds assembling giant molecular clouds (GMCs).**

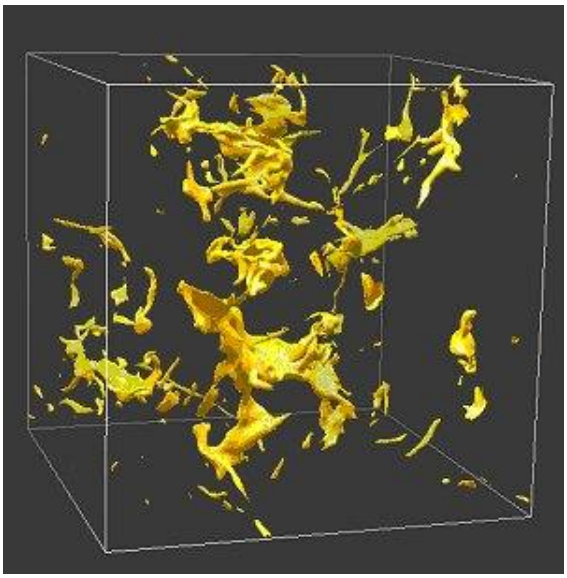

Figure 6: The ISM is a complex environment with structures on all scales and velocity dispersions. The surfaces of clouds corresponding to $n = 30$ cm^{-3} are shown within a 6 pc region from a 3-D magnetohydrodynamical simulation of cloud formation (Juvela et al., 2003). Neither COBE nor BICE had the spatial and spectral resolution to unravel the structure of the interstellar clouds or their formation process.

Turbulence may play an important role in the formation and evolution of interstellar clouds. In a standard scenario where CNM clouds are formed from WNM gas by thermal instability, we can picture the role of turbulence in two ways: large scale instabilities, density waves and supernovae drive compressional motions that can trigger the thermal instability (de Avillez & Breitschwerdt, 2005). Alternatively, regions undergoing thermal instability experience a dynamic radiative transition from the WNM to the CNM, due to the large density contrast between these two phases. This transition is known to generate turbulence and to set up the CNM into a complex network of pancakes and filaments (Kritsuk & Norman, 2002, also Figure 6). Because of this dynamic nature of both the triggering and evolution of the thermal instability, departures from thermal pressure equilibrium may be widespread in the ISM (Heiles & Troland, 2003), and the notion of a dynamic multiphase ISM has been proposed, where turbulent diffusion regulates phase exchange processes. Only a careful study of both the spatial structure and kinematics of gas in transition between phases can tell us the role of turbulence and dynamic pressure in the life-cycle of the ISM.

Other theories of (molecular) cloud formation are also guided and constrained by observations of the atomic and molecular gas components. Four mechanisms have been proposed to consolidate gas into GMC complexes (Figure 7): (1) self-gravitating instabilities (Kim & Ostriker 2002,2007) within the diffuse gas component (often in a spiral arm where density is highest and the Jeans time is shortest), (2) collisional agglomeration of small, long-lived molecular clouds, (3) accumulation of material within high pressure environments such as shells and rings generated by OB associations, and (4) compression in the randomly converging parts of a turbulent medium. STO can distinguish these processes from each other and consider new cloud formation schemes by:

- Accounting for all the molecular hydrogen mass (the H_2/C^+ clouds as well as the H_2/CO clouds) when computing global measures of the interstellar medium.
- Making a more complete, better characterized catalogue of interstellar clouds than CO or H I surveys.
- Constructing spatial and kinematic comparisons with sufficient resolution, spatial coverage and dynamic range to probe a wide range of interstellar phases and environments.

Currently, associating diffuse gas (H I) with molecular gas (CO) is difficult owing to the large differences of emitting volumes of the H I line and the CO line (see Figure 8). Unlike [C II], a significant fraction of the H I emission can come from low density WNM gas. [C II] emission barometrically picks out clouds of atomic CNM gas and H_2 clouds with little CO. Regions of GMC formation may therefore be tracked by higher than average cloud densities (number of clouds per kpc^3), or regions with individual clouds with higher than average columns or pressures. With STOs velocity resolution, these regions can be identified with superrings or spiral arms or convergent parts of a turbulent medium.

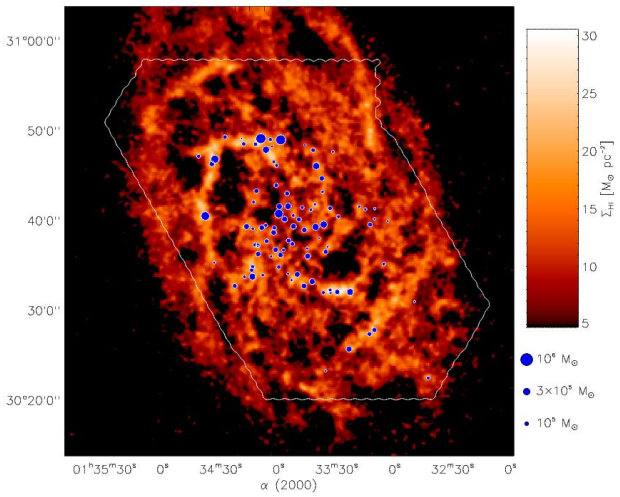

Figure 7: The location of GMCs in the nearby spiral galaxy M33 are overlaid upon an integrated intensity map of the H I 21 cm line (Engargiola et al., 2003). These observations show that GMCs are formed from large structures of atomic gas, and foreshadow the detailed study of GMC formation that STO provides in the Milky Way.

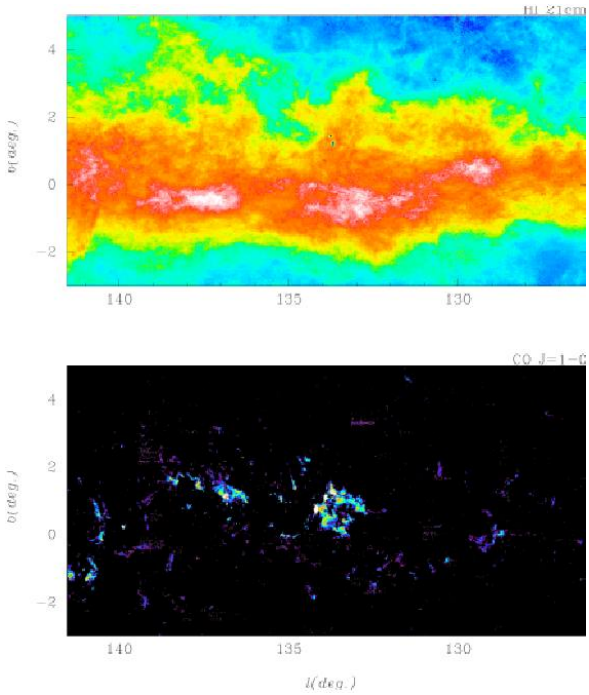

Figure 8: The integrated 21 cm line (top) and CO J=1-0 (bottom) emission from the Perseus spiral arm. The H I and ^{12}CO data are from the Canadian Galactic Plane Survey (Taylor et al., 2003) and the Five College Radio Astronomy Observatory CO Survey of the Outer Galaxy (Heyer et al., 1998), respectively. STO enables a more direct comparison of diffuse gas with the underlying molecular cloud.

STO will identify the sequence of phase transitions as the gas transits through the spiral potential, and *will witness the process of cloud formation* directly from the atomic substrate or from small H_2 clouds. For example, dust lanes along the inner edges of spiral arms often show neither H I nor CO emission (Wiklind et al., 1990; Tilanus & Allen, 1991), and are therefore likely to be in an intermediate phase; sufficiently dense and self-shielded to harbor H_2 but not CO (Grenier et al. 2005, see also Figure 3). These clouds will be seen in [C II] by STO.

The high spectral resolution of STO enables crucial kinematic studies of the Galaxy to be made. The expansion of stellar outflows and supernova remnants create supershells that sweep up surrounding ISM and overrun surviving molecular clouds and cloud fragments. The high pressures in the shells convert swept-up WNM gas to CNM clouds via thermal instability. The resulting supershell can grow to several times the typical thickness of the gas layer in a galactic disk, creating superrings that can contain millions of solar masses of swept-up gas. Gravitational fragmentation of superrings may be an important mechanism for the formation of GMCs (Elmegreen, 1989; McCray & Kafatos, 1987).

STO will determine the kinematics and thermal pressures of most supershells, fossil superrings, and molecular clouds just condensing via gravitational instability of old superrings. STO will detect many of the CNM clouds formed out of WNM in the shells, and the larger column density clouds, which may harbor H_2. With these detections STO will determine the role of OB association-driven supershells and superrings in the production of molecular clouds and the cycling of gas between the various phases of the ISM.

STO witnesses the disruption of clouds: [C II] and [N II] measure the photoevaporating atomic or ionized gas driven from clouds with UV-illuminated surfaces, thereby converting the clouds to WNM or to diffuse H II regions. Thus, STO can directly determine the rate of mass loss from all catalogued clouds, and their destruction timescales.

Goal 3: Star Formation Rate in the Galaxy

Star formation within galaxies is commonly described by two empirical relationships: the variation of the star formation rate per unit area with the gas surface density (atomic + molecular), $\Sigma_{\rm SFR} \sim \Sigma_{\rm gas}^n$

(Schmidt, 1959) and a surface density threshold below which star formation is suppressed (Kennicutt, 1989; Martin & Kennicutt, 2001). The Schmidt Law has been evaluated from the radial profiles of Hα, H I, and CO emissions for tens of galaxies. The mean value of the Schmidt index, n, is 1.3 ± 0.3 (Kennicutt, 1989), valid for kpc scales. This empirical relationship is used in most models of galaxy evolution with surprising success given its simplicity. Oddly, there has been little effort to evaluate the Schmidt Law in the Milky Way owing to the difficulty in deriving the star formation rate as a function of radius within the plane.

The STO survey of [C II] and [N II] emission provides the optimum set of data to calculate the Schmidt Law in the Milky Way. The [N II] line is an excellent tracer of the star formation rate as it measures ionizing luminosity with unmatched sensitivity, angular and spectral resolution, and is unaffected by extinction. The [C II] line, in conjunction with H I 21-cm and CO line emissions, provide the first coherent map of the neutral interstellar gas surface density and its variation with radius.

STO may help us understand the origin of the Schmidt Law. For example, it will correlate the thermal pressures on the surfaces of GMCs (which may relate to the star formation rate inside) with surface densities of H I and CO. It may uncover regions around OB associations devoid of GMC-forming CNM clouds. The current high rate of star formation in associations may impoverish large regions of the clouds needed to start the star formation cycle in the future. Such measurements are pivotal to models of star formation feedback & global galactic evolution.

Goal 4: The Milky Way Template

[C II] 158 μm, the strongest Galactic cooling line, will be the premier diagnostic tool for studying external galaxies with future far-infrared (FIR) observatories (SOFIA, Herschel) and in the submillimeter for galaxies with large redshifts (Atacama Large Millimeter Array). In such spatially unresolved galaxies, however, only global properties can be measured. To interpret the measurement of extragalactic [C II] one must turn to the Milky Way for the spatial resolution needed to disentangle the various contributors to the total [C II] emission. At present, there is debate on the dominant origin of the [C II] emission in the Galaxy: diffuse H II regions, CNM clouds, or the surfaces of GMCs. STO will solve this mystery. The [C II] and [N II] intensities depend on the strength of the UV heating and on the amount of gas in the appropriate ISM phase. The STO mission covers a broad range of density and UV intensity, thus establishing the relationship between physical properties, [C II], [N II], CO, H I, FIR emission, and star formation. This study will provide the "Rosetta Stone" for translating the global properties of distant galaxies into reliable estimators of star formation rate and state of the ISM.

Possible Additional STO Flights

STO, as a balloon-borne mission, has the great potential to be reflown, possibly with new receiver modules that enable different spectral lines to be surveyed. The first flight is designed for the science described in previous sections and focuses on the Galactic disk between 3 kpc and 8.5 kpc. However, there are a number of extremely interesting scientific goals that could be met on subsequent flights. We briefly list here a possible sequence of flights to give the flavor of this enormous potential.

Flight 2. Flight 2 could map [C II] and [N II] in the very interesting center of the Galaxy, as well as conducting deep maps directed towards the outer galaxy. The compressed and turbulent interstellar medium of galactic nuclei provides a completely different environment for star formation than the relatively quiescent disk. STO could explore the Galactic Center with sufficient spatial ($\sim$3 pc) and spectral resolution to separate large clouds and trace material as it falls into and through the center region. STO could study the origin of the mysteriously low [C II]/FIR flux ratio (Nakagawa et al., 1998), all of the center's massive cloud complexes, and the bar. High-velocity resolution observations will provide a new kinematic map of the gas, ultraviolet fields, and star formation in the nucleus.

The outer Galaxy provides a testing ground for understanding cloud formation and star formation in lower surface density and lower metallicity environments. STO will answer what determines the threshold in gas surface density which causes massive star formation to rapidly diminish.

Flight 3. Flight 3 could allow us to change wavelengths, and pursue the [O I] 63 μm or 145 μm line as well as the [N II] 122 μm line. These lines increase in strength in dense gas and we envision deep surveys in regions selected by our flights 1 and 2. The [O I] maps will "light up" the regions of higher thermal pressures (or densities) and higher incident UV fields, like the surfaces of GMCs. Combined with the [C II] line, [O I] constrains these diagnos-

tics of star forming clouds. In addition, warm cores are bright background continuum sources towards which [O I] 63 μm line absorption can be observed (e.g. Vastel et al. 2002). Such observations will address a key puzzle in our understanding of the oxygen budget in dark clouds; is oxygen present in the gas phase, or is it largely depleted onto icy grain mantles?

The [N II] 122 μm line, combined with the [N II] 205 μm line from previous flights, gives a measure of the electron density (n_e) in H II regions, and therefore the thermal pressure in ionized gas. The electron density enables us to check our measurement of the star formation rate by [N II] 205 μm, since at high density ($n_e > 100$ cm^{-3}), it is the [N II] 205 μm luminosity times n_e which scales as the star formation rate.

Flight 4. Another change of wavelength could bring the ground state rotational line of HD at 112 μm into view. This line would principally be detected toward the sites of massive star formation, so many targeted pointings would be planned. Combined with observations of the dust continuum and other molecules, the HD line would provide a measure of the deuterium abundance in molecular gas. When compared to theoretical models of deuterium destruction by astration, previous UV observations of DI and mid-IR observations of HD (Neufeld et al. 2006) have yielded elemental D abundances that are both surprisingly small and variable, a discrepancy which may indicate that interstellar deuterium might be significantly depleted onto large aromatic hydrocarbons (Linsky et al. 2006). STO observations of HD J=1-0 will provide two important advantages over current mid-IR observations: they will probe cold molecular clouds in which mid-IR HD transitions are not excited, and provide enough spectral resolution to discriminate between multiple clouds along a given sight-line.

4 Science Requirements

4.1 *High Resolution Spectroscopy*

The superposition of many clouds along the line of sight can be disentangled with spectral line techniques. Fitting to a model of Galactic rotation is often the only way to determine each cloud's distance and location within the Galaxy. It is the spectral resolution that gives us a 3D rather than a projected 2D map of the Galaxy. Moreover, internal dynamics are revealed from the variance of measured velocities and profile line widths within interstellar clouds. With resolution finer than 1 km s^{-1}, a line profile can disentangle processes such as turbulence, rotation, and local effects such as protostellar outflows. These kinematic components play a vital role in the sculpting of interstellar clouds, and a survey that has the goal of understanding their evolution **must** be able to separate the velocity components.

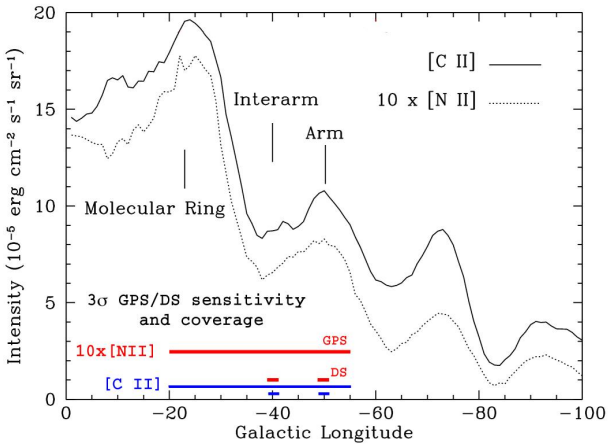

Figure 9: [C II] and [N II] intensity in the Galactic plane seen in the COBE beam (Steiman-Cameron et al., 2007). STO's sensitivity to [NII] (red) and [CII] (blue) and coverage of the Galactic Plane in its two survey modes is shown. Note that this sensitivity is obtained while simultaneously providing unparalled velocity and angular resolution.

4.2 *Large Scale Mapping*

Interstellar pressure, elemental abundances, and radiation field vary as a function of Galactic radius, so it is necessary to probe from the inner Galaxy out to at least the solar circle to obtain a statistically meaningful survey that encompasses the broad dynamic range of conditions in the Galaxy. Large cloud ensembles, as gathered by surveys, are required to average properties extracted from clouds at varying stages of evolution. Large scale mapping places detected interstellar structures in an environmental context. To meet these objectives we will carry out an unbiased Galactic plane survey (GPS), and deep surveys (DS) of selected areas in the Galactic plane.

Galactic Plane Survey (GPS)

This moderate sensitivity survey will sample the Galactic plane at longitudes $-20° > l > -55°$ and $0° < b < 1°$ in 12 second integrations per convolved 1.5′ beam. This survey region crosses the molecular ring ($l \sim -23°$), spiral arm regions ($l \sim -50°$), and

interarm regions ($l \sim -40°$). The molecular ring, arm, and interarm environments are clearly identified in both [C II] and [N II] emission in the COBE 7° beam (Figure 9). In addition, numerous shells, bubbles, and star formation regions appear throughout our survey area as seen, for example, on MSX 8μm emission maps (Figure 2). Thus, our survey probes the Galactic regions where the full cycle of cloud formation and destruction occurs.

Deep Surveys (DS)

The deep sensitivity survey will consist of observations at 90 seconds of integration per 1′ beam towards arm ($l \sim -50°$) and interarm regions ($l \sim -40°$) in the GPS shallower survey region. These maps cover a total area of one square degree and include the Scutum-Crux arm (seen in H II regions, ionized gas, [N II] and [C II]) and the adjacent interarm region between Scutum-Crux and the molecular ring. The GPS survey only allows detection of clouds with columns of $A_V \geq 0.4$, and so only uncovers the most massive CNM diffuse clouds. Our deep surveys allow a much broader range of diffuse clouds to be studied, down to a column $A_V \sim 0.1$. In addition, for fixed A_V, CNM clouds in lower pressure regions, or in regions with lower heating rates are more difficult to detect. Deep surveys therefore also extend our ability to detect clouds along the line of sight in such regions.

4.3 Angular Resolution and Full Sampled Maps

Previous surveys of [N II] and [C II] were limited to very small regions (KAO, ISO) or had low angular resolution (COBE, BICE) (Bennett et al., 1994; Nakagawa et al., 1998). STO will fully sample both species over large regions of sky to their diffraction limited resolution of 1.1′ and 0.8′, respectively. Arcminute resolution with proper sampling is crucial to disentangling different clouds and cloud components over large distances in the Galaxy. At a distance of 10 kpc, GMCs subtend 10′, CNM clouds or small molecular clouds subtend 1-2′, diffuse H II regions about 20′. Such diffuse H II regions tend to dominate [N II] and [C II] emission from ionized gas (McKee & Williams, 1997) and are a substantial component of the ionized gas in the Galaxy.

4.4 High Sensitivity

Figure 4 shows the required STO sensitivity for detecting [C II] and [N II] from photodissociated cloud surfaces and for distant (∼10 kpc) clouds in the inner Galaxy. Our most demanding requirements lie in the search for the formation of molecular clouds and the measurement of the warm ionized medium in the Galaxy. A flux limit of 10^{-6} erg s^{-1} cm^{-2} sr^{-1} will detect [N II] in diffuse H II regions as far away as the Molecular Ring, achievable in 12 seconds of integration with velocity smoothing to 5 km s^{-1}, appropriate for ionized gas. Tracing the formation of GMCs requires the detection of cold neutral clouds of relatively low column densities of $\sim 5 \times 10^{20}$ cm^{-2}. The expected [C II] emission at high interstellar pressures would be 10^{-5} erg s^{-1} cm^{-2} sr^{-1}, detectable in 8 seconds with STO. The STO Deep Survey allows the study of smaller columns of gas, and/or regions of lower interstellar pressure, such as in the Solar vicinity.

5 Complementarity with Existing Data Sets and Other Missions

STO will provide the community with a totally unique [C II] and [N II] survey, enabling quantitative extraction of many physical parameters of the interstellar medium in a 3D data cube. Its spatial resolution exceeds Galactic Plane surveys of CO emission in the southern hemisphere (Dame et al., 2001; Onishi et al., 2005) and is comparable to the Southern Galactic Plane HI Survey (McClure-Griffiths, 2005), allowing placement of the [C II] 158 μm and [N II] 205 μm emission along the line of sight with respect to the CO and H I emission.

5.1 Relationship to Existing Data Sets

CO: For tenuous clouds of column less than about $N < 2 \times 10^{21}$ cm^{-2}, the CO is photodissociated and the CO emission either disappears entirely, or if present, is a very unreliable measure of the molecular mass. The more opaque clouds in the 5×10^{20} to 3×10^{21} cm^{-2} range may be primarily H_2, which is extremely difficult to detect directly. These clouds have most of the carbon in C^+, which makes [C II] the only reliable probe. [C II] not only detects the CO clouds (via the emission from their C^+ surfaces), but also the H_2 clouds at intermediate column, and the mainly atomic clouds with $N < 5 \times 10^{20}$ cm^{-2}. Recent J-K extinction maps (Figure 10) confirm these components are present. Thus, the [C II] detects a broader range of clouds than the CO, and allows us to see the possible assemblage of clouds of ever greater column, from atomic clouds, to H_2 clouds, to CO clouds.

The CO surveys will complement the STO survey by helping to identify molecular clouds whose

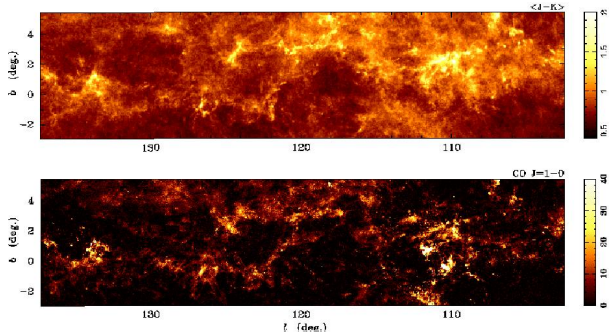

Figure 10: Near infrared $J-K$ extinction maps (top) depict significant interstellar gas not probed by CO (bottom). [C II] line emission will barometrically select young molecular clouds that have formed H_2 but not CO.

surfaces STO detects and whose ionized gas seen in [N II] may be expanding into the ISM (Dame et al., 2001; Onishi et al., 2005).

H I: The STO surveys enhance substantially the interpretation of existing H I surveys. The H I emission maps are sensitive only to column, whereas [C II] is sensitive to density times column. The [C II] therefore picks out the cloud regions with density $>$ 30 cm^{-3}, whereas the H I is often dominated by the WNM emission (see Figure 5). In fact, H I clouds can appear in absorption, in emission or undetected against the confused background and foreground WNM. When H I and [C II] are both seen in emission, the ratio provides the gas density and pressure in the cloud. When extended and broad H I emission is seen without a [C II] counterpart, WNM or thermally unstable gas is identified. For H I, the relevant dataset for STO is the Southern Galactic Plane Survey with 1′ resolution (McClure-Griffiths, 2005).

[C I]: Moving from the CNM through the surfaces of molecular clouds to their cores, the predominant form of carbon transitions from C^+ to CO, with high abundances of C in the transition region. Unbiased surveys of the [C I] fine structure lines, with parameters similar to the STO survey, have recently become feasible (Martin et al., 2004; Zhang et al., 2001). Maps from STO coupled with CO and [C I] data, will follow carbon in all its forms in position, velocity, cooling rate, temperature and pressure as the interstellar gas evolves.

Infrared Continuum Surveys: MSX, Infrared Astronomical Satellite (IRAS), and Spitzer GLIMPSE and MIPSGAL Galactic plane surveys permit locating dark clouds, supershells, and star forming regions using the IR continuum.

5.2 *Complementarity to Other Missions*

STO builds upon the heritage of three pioneering surveys which provided coarse pictures of [C II] and [N II] emission in the Galaxy. COBE (spatial resolution 7°, velocity resolution >1000 km/s), BICE (spatial resolution 15′, velocity resolution 175 km/s), and the Infrared Telescope in Space (IRTS, spatial resolution 10′, velocity resolution 750 km/s). *STO has about the same sensitivity to surface brightness as these missions, but adds orders of magnitude in spatial and spectral resolution.* None of these missions had sufficient spectral or spatial resolution to locate clouds, or separate one cloud from another along a given line of sight, and thus could not draw specific conclusions about cloud properties or distributions, or even the origin of the [C II] or [N II] emission (Hollenbach & Tielens, 1999).

Besides COBE, BICE and IRTS, other platforms include the now defunct Kuiper Astronomical Observatory and Infrared Space Observatory, which did not survey the Galaxy in [C II] and [N II], but made pointed observations. The Spitzer Space Telescope has no spectroscopic capability at these wavelengths. Herschel's HIFI instrument (2009-2013) and (SOFIA, 2009+) will have the capability to observe both [C II] and [N II] at high spectral resolution. The advantage of STO, however, is its ability to provide large scale coverage. Herschel and SOFIA are complementary to STO in providing higher angular resolutions at the [C II] and [N II] lines, $\sim 10''$ as compared to STO's $60''$. Given that Herschel's [SOFIA's] beam covers an area 2% [4%] the area of STO's beam, there will not be sufficient time on these other facilities to complete even a small fraction of the Nyquist-sampled Galactic survey of the scale proposed for STO. Indeed, Herschel & SOFIA are general purpose observatories with a variety of instruments and science goals. We estimate that each facility will map only a few percent of the area of STO's survey in the [C II] and [N II] lines with heterodyne instruments during their lifetimes. It is important that these higher spatial resolution maps be well chosen and STO can provide guidance.

6 Science Implementation

6.1 *Instrument Summary*

The observational goal of STO is to make high spectral (<1 km/s) and angular resolution (∼1 arcminute) maps of the Galactic plane in two astro-

physically important atomic transitions: [N II] at 1.5 THz (205 μm) and [C II] at 1.9 THz (158 μm). To achieve the angular resolution requirement we have designed STO to utilize an aperture of 80 cm. To achieve the target spectral resolution, STO will utilize a heterodyne receiver system. STO will be a long duration, balloon-borne observatory which will be launched from McMurdo, Antarctica to an altitude of 120,000 ft, where it will remain for 10-14 days. The instrument portion of STO consists of (1) the telescope, (2) eight heterodyne receivers: four at the 1.5 THz [N II] line and four at the 1.9 THz [C II] line, (3) an eight-channel FFT spectrometer system, (4) the instrument control electronics, (5) the hybrid ^{4}He cryostat, and (6) the gondola.

Requirement	**Specification**
Telescope:	
Aperture	0.8m
Type	on-axis Cassegrain
Spectral Range	60 to 210 μm
Pointing Knowledge	$\sim 15''$
Chopper Throw	$\pm 0.4^\circ$ @ $\sim$1 Hz
Receiver:	
Target Frequencies	[C II]1.901 THz
	[N II]1.461 THz
Angular Resolution	$\sim 1'$
Receiver Type	4-pixel HEB Mixer Arrays
Receiver Noise	$\sim$1500K (DSB)
Spectrometer:	
Type	8x1 GHz FFT analyzers
Bandwidth	1 GHz (160-205 km s^{-1})
Resolution	1 MHz (0.2 km s^{-1})
Cryogenic System	
Type	^{4}He+60K cryocooler
Hold time	$>$14 days

Table 1: Key Instrument Parameters for STO

The STO gondola is based on previous successful JHU/Applied Physics Laboratory (APL) designs and includes (1) the solar arrays and power regulation system, (2) the attitude control system, and (3) NASA-CSBF command & telemetry system. The primary science mission of STO will be achieved in the first 10 days of flight. STO will benefit tremendously from hot electron bolometer (HEB) mixer and solid-state LO technology that has been developed in support of the Herschel mission. The focal plane will be cooled to 4K by a simple ^{4}He cryostat with a mechanical cryocooler to cool radiation shields to $<$60K to maximize helium hold time while minimizing instrument mass.

6.1.1 STO Telescope

The scientific program for the STO requires that the telescope optics allow a large beam throw ($\sim \pm 0.4^\circ$) out of the Galactic Plane at a speed of $\sim$1 Hz.

For STO we use the same telescope that APL previously employed for its successful balloon instrument the Flare Genesis Experiment (FGE) (Bernasconi et al., 2000) depicted in Figures 11 and 17. The telescope was originally developed by the Strategic Defense Initiative Organization (SDIO) for the Starlab program. Subsequently, it was acquired by APL and modified to fit the science objectives of FGE. The primary mirror is an 80-cm diameter, f/1.5 hyperboloid made of Ultra Low Expansion titanium silicate glass (ULE), and honeycombed to a weight of just 50 Kg. Its surface is polished to visible optical quality, therefore over-specified for imaging in the 100 to 200 μm range. Its support and spider arms are made of graphite-epoxy, which is very light weight, and provides high thermal stability over a wide range of temperatures. Figure 11 shows the FGE telescope during a Sun pointing test session. The same telescope will be used for STO with only minor modifications.

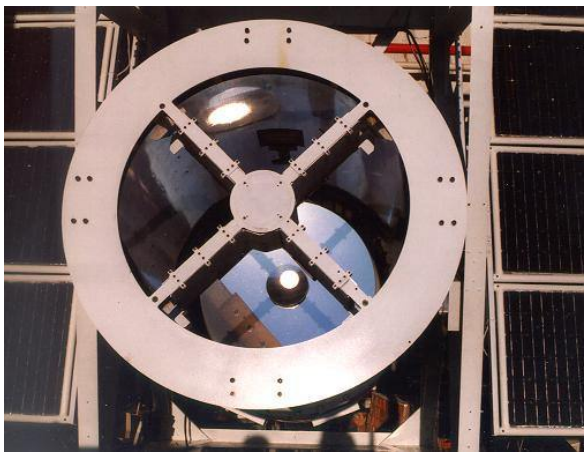

Figure 11: The Flare Genesis telescope while pointing at the Sun

For STO the secondary mirror is redesigned to provide an f/7 beam in the focal plane. The secondary is machined from solid aluminum, with an rms surface accuracy of $<$4 μm. It is light weighted by machining pockets in the back. The tertiary chopper is located near the back side of the main

mirror on a counterbalanced mount to minimize reaction forces. The secondary is oversized so that spillover does not change significantly as a function of chopper throw.

There is a small calibration box located between the telescope and the receiver dewar. This subsystem places blackbody loads at known temperatures in the path of the detectors using linear actuators and moving mirrors. One of the loads is allowed to come into thermal equilibrium with the temperature of the surrounding air: its temperature is monitored by an embedded RTD and recorded. Another load is located on the 60K stage of the receiver dewar. Periodic measurements of the power radiated from these loads allow determination of the detector gain. The power from these loads will also be compared to the variation in power resulting from a change in telescope elevation: a skydip. These measurements suffice to determine the detector noise, the telescope efficiency, and the opacity of the atmosphere and the absolute flux of astronomical sources (Ulich & Haas, 1976).

6.1.2 Receiver Description

The design of the receiver leverages strongly off experience gained by the PI and Co-I's in constructing numerous receiver systems. These receivers have served as facility instruments on the Caltech Submillimeter Observatory (CSO), the University of Arizona Submillimeter Telescope (SMT), the Antarctic Submillimeter Telescope and Remote Observatory (AST/RO), and the SAO Receiver Lab THz Telescope (RLT). A cut-away view of the STO cryostat showing the placement of the receiver system is shown in Figure 12. A diagram showing integration with the telescope is shown in Figure 13a and a block diagram of the instrument in Figure 13b.

The f/7 telescope beam first encounters a free-standing wire grid that divides the incident light into horizontal and vertical polarization components. One polarization passes through the grid into the first vacuum window. The other polarization reflects off a 45° mirror and enters a second vacuum window. The vacuum windows and subsequent 60 and 4 K IR filters are made from low-loss, AR coated, single crystal quartz. The first flight receiver will consist of two, orthogonally polarized 1x4 arrays of superconductive hot-electron bolometer (HEB) mixers operating at 4K. One array is optimized for the [C II] (1.90 THz) line, the other for the [N II] (1.46 THz) line. The mixers will be pumped by two, frequency tunable, solid-state Local Oscillators (LO's). The final multiplier stage is mounted to the

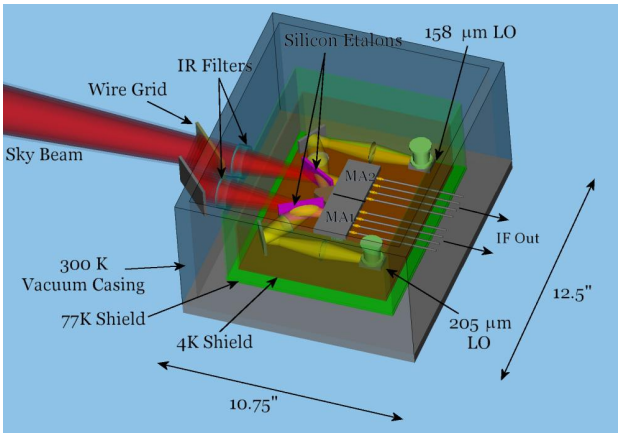

Figure 12: 3-D cutaway rendering of the flight instrument cryostat

4 K cold plate via G-10 stand-offs to the 60K stage. At this temperature the multiplier emits approximately twice the power it would at ambient temperatures. An integrated, waveguide power splitter at the output of each multiplier efficiently divides the LO power four ways and couples it via a silicon etalon into each mixer. The silicon etalon is designed to pass $\sim 95\%$ of the sky signal and reflect $\sim 68\%$ of the LO signal (Mueller & Waldman, 1994).

Low-noise, InP High Electron Mobility Transistors (HEMT) amplifiers are integrated into each array mixer and serve as the first stage intermediate frequency (IF) amplifiers (Puetz et al. 2006). The IF center frequency will be $\sim$2 GHz, with an instantaneous bandwidth of $\sim$1 GHz. This IF frequency and bandwidth can be supported by NbN phonon-cooled mixers. At our highest observing frequency (1.9 THz, the [C II] line) a 1 GHz IF bandwidth will provide 160 km/s of velocity coverage. A velocity coverage of this order is needed to accommodate the wide velocity dispersion expected toward the inner parts of the Galaxy. Doppler tracking of the LO frequency will keep the received signal centered within the IF band. The eight IF signals from the mixers pass through an ambient temperature IF processor where they are further amplified and down-converted to baseband (0-1 GHz). STO will use eight 1 GHz wide, 1024 channel digital FFT analyzers as backend spectrometers for the mixer arrays. A flight instrument electronics box will house (1) the IF processor board, (2) the 8x1 GHz spectrometer boards, (2) the LO/HEB/LNA bias board, (4) calibration flip mirror controller board, and (5) the Instrument Computer. The Instrument Computer communicates to the Gondola computer via an RS-

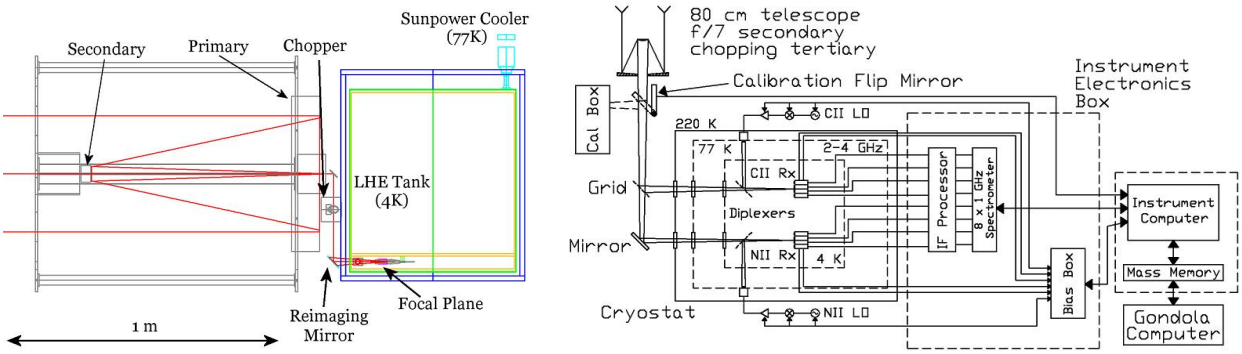

Figure 13: (a) Instrument and telescope integration configuration, demonstrating how the complete STO instrument will fit into the payload footprint of the previous Flare Genesis instrument. (b) Block diagram of the instrument flight package.

422 bus. Prototype versions of all boards exist.

6.1.3 *Expected Sensitivity*

Recent lab measurements on waveguide and quasi-optical HEBs in the 1 to 2 THz range have yielded double side band (DSB) receiver noise temperatures in the 1000-2000K range. For our sensitivity calculations we have assumed a receiver noise temperature of 1000-1500K and T_{sys} = 2000-3000K. With the 12 second integration time per Nyquist-sampled resolution element characteristic of the unbiased, Galactic Plane survey (GPS) mode, we will be able to achieve an rms noise level of 0.4 K at a 1 km/s velocity resolution. The STO instrument characteristics are summarized in Table 1.

6.1.4 *Component Selection*

Technical Approach to Mixers

HEB mixers (both in the lab and in the field) have been shown to have the sensitivity needed for the proposed STO science investigations. The STO mixer design follows the very successful and practical HEB instruments that were developed by the submillimeter receiver groups at the Smithsonian Astrophysical Observatory (SAO) and the University of Cologne. A plot of the noise temperature of these HEB receivers as a function of frequency is shown in Figure 14a. JPL/SAO has tested receivers up to 1.5 THz and the Cologne group up to 1.9 THz. The SAO instrument has been used on a telescope in the high Atacama over a two-year period and used to detect line emission from celestial sources from 0.69 THz to 1.46 THz. A University of Cologne receiver was also field tested in this frequency range on a telescope in the Atacama. Transitioning these superconductive HEB mixers to a gondola instrument will be straight forward. The mixers utilize a fixed-tuned waveguide design with high efficiency feedhorns. Traditional machining methods are used to fabricate the mixer blocks. The mixer circuitry, including the mixer element, waveguide probe and choke structure, is fabricated on a thin substrate which is laid in a suspended microstrip channel intersecting reduced-height waveguide (see Figure 14b). Using SOI substrates for the HEBs, this type of mixer can be scaled for operation to 4.7 THz (the 63 μm [OI] line). HEB mixer operation has been demonstrated to frequencies above 5 THz (Gao et al., 2004).

The 1x4, 1.46 THz array will be provided by JPL and the 1x4, 1.9 THz array by the Univ. of Cologne.

Technical Approach for the LO hardware

The 1.46 and 1.9 THz solid-state local oscillator sources required for the first flight instrument are commercially available from Virginia Diodes Inc. (see Figure 15). The LO's have a tuning range suitable for Doppler tracking of sources and have sufficient output power when cooled to pump the array mixers. The LO chains are driven by small, low-cost, programmable 13-15 GHz synthesizers which are available, for example, from CTI/Herley. The Instrument Computer will routinely update the synthesizer frequency to maintain Doppler tracking during observations.

Solid state LO's as described here do not provide sufficient power to drive arrays of mixers above ~2 THz. Fortunately, in this frequency regime quantum cascade lasers (QCLs) (Hu et al. 2005) and compact gas lasers (Mueller 2006) can be fabricated that provide more than enough power to drive HEB arrays for future STO flights.

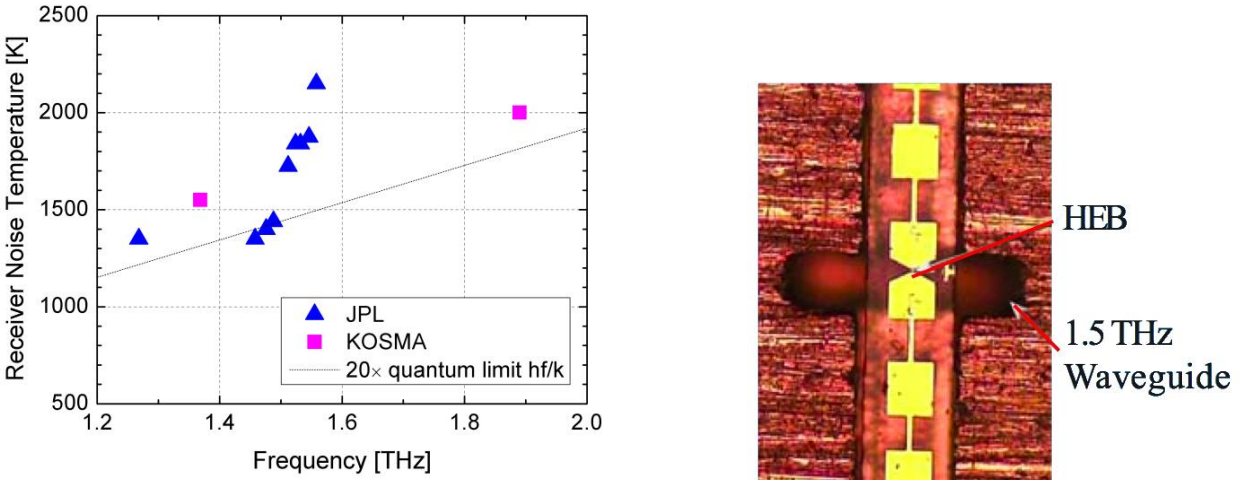

Figure 14: (a) THz HEB mixer performance from SAO using JPL-supplied NbTiN mixers and the University of Cologne. (b) SAO waveguide HEB implementation

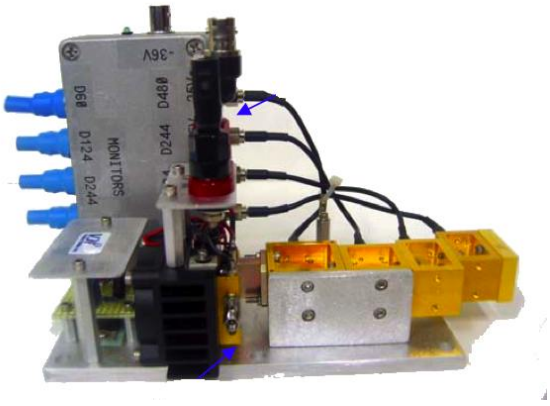

Figure 15: Virginia Diodes 1.5 THz synthesizer driven local oscillator chain

Figure 16: The assembled 16 GHz FFT spectrometer from the PI's Supercam project is no larger than a rack-mounted PC! The equivalent of half of this spectrometer will be purchased for STO.

6.1.5 Digital Spectrometer

Thanks to rapid advances in digital processing, single-board digital spectrometers that meet STO's requirements are now commercially available. One such spectrometer board is available from Omnisys Inc. Developed originally for the PI's 64-beam 345 GHz heterodyne array ("SuperCam") project, the Omnisys board has four 1 Gs, 8-bit digitizers and a Xilinx Virtex4 FPGA which together perform a realtime FFT of the IF signal. The baseline spectrometer card has 2 GHz of total bandwidth and achieves excellent performance and stability. A picture of the delivered 16 GHz spectrometer system for SuperCam is shown in Figure 16. Four Omnisys boards will be baselined for STO, providing 8 IF inputs with 1 GHz of bandwidth each. The demonstrated power dissipation of the complete 8 x 1 GHz spectrometer system is <100W.

6.1.6 Cryogenic System

The STO flight cryostat will use liquid ^{4}He to cool the instrument to the required operating temperatures. An off-the-shelf mechanical cryocooler will cool the radiation shields to 60K to give the 4K helium stage a >14 day holdtime. The flight cryostat is based on a thin wall cylinder design that utilizes stiffening rings located at critical segment interfaces. A finite element analysis will determine actual material thickness from acceleration data typical for a gondola payload. Certificate compliance forms will trace all materials and fabrication used in manufacturing the cryostat. The internal support structure will use G10 supports to maintain stiffness and allow for thermal contraction. The cryostat will have an aluminum case with welded internal vessel and use high performance vapor shields to enclose

the inner ^{4}He vessel.

6.2 STO Gondola

6.2.1 Heritage

The STO program will build upon the 15 years experience in ballooning resident at APL. In the early 1990s, APL started developing a balloon system for the NASA funded Flare Genesis Experiment (Figure 17) to conduct high spatial resolution solar vector polarimetric imaging (Bernasconi et al., 2000). FGE required high stability pointing on the order of a few arc seconds. APL developed a balloon attitude control system that was able to point at the Sun with an accuracy of 20″ and a stability of <8″ RMS. Subsequently, APL used the same gondola and attitude system with the Solar Bolometric Imager (SBI) for conducting solar irradiance studies (Bernasconi et al., 2004). SBI was also funded in most part by NASA. Both efforts heavily involved APL's space department engineering group as well as the APL Technical Services Department. This pool of expertise will be utilized in the implementation of STO. Mr. Harry Eaton of TSD will be the gondola lead systems engineer. Mr. Eaton is a very experienced electrical engineer who contributed to all APL balloon programs since the mid 1990s and is currently the lead engineer for the SBI program.

Figure 17: APL's Flare Genesis gondola during integration tests in Palestine, TX in 1999.

6.2.2 Gondola Structure

The STO observing platform (gondola), shown in Figure 18, is the one previously used by APL for its FGE (Figure 17) and SBI balloon programs. The gondola has successfully endured two test flights in New Mexico (in 1994 and 2003) and three Antarctic flights (in 1996, 2000, and 2006). During the past ten years the gondola and its subsystems have undergone many improvements and upgrades. The STO project will benefit directly from this flight heritage. There is no need to design, manufacture and test a new gondola.

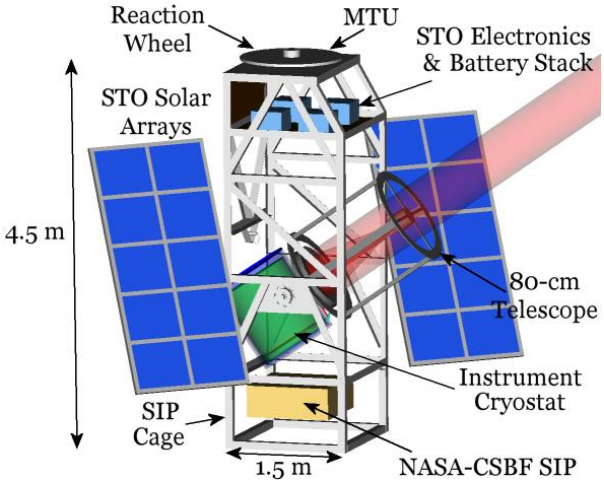

Figure 18: 3-D rendering of the gondola package, including 80-cm telescope and science payload.

The gondola carries and protects the telescope and attached Dewar and detectors, houses the command and control systems for both STO and NASA-CSBF, and the power system. Its basic dimensions (without solar arrays) are: 2m wide, 1.5m deep, and 4.5m high. The frame is made of standard aluminum angles bolted together and painted with a white thermal coating. The structure is strong enough to support up to 2000 Kg even under the 10 g shock experienced at the end of the flight when the parachute inflates. It is rigid enough to allow the required telescope pointing stability of <15″. The gondola can be separated into lighter components for easy post-flight retrieval in the field.

The gondola structural and servo systems are designed for the estimated masses shown in Table 2. The total mass of the STO payload is well below the design structural limit of the APL gondola.

NASA-CSBF balloon command and control electronics (the Support Instrument Package, SIP) is attached below the telescope, inside a protective alu-

Item	Weight lbs	Kg
Gondola with command & control:	2200	998
Telescope:	200	91
Heterodyne spectrometer/He dewar:	200	91
CSBF Equipment:	570	258
Ballast allotment:	600	272
Total:	3770	1710

Table 2: Launch weights estimates for STO payload.

minum cage the same way it was for FGE and SBI. Communications from the SIP to the balloon and parachute control mechanism are guaranteed via slip rings through the rotating part of the Momentum Transfer Unit on top of the gondola. APL will use the same slip rings successfully tested for the FGE and SBI programs.

APL already has detailed thermal and structural models for the current configuration of the APL gondola. The models will be modified to take into consideration the mechanical and electronics changes necessary to fit the STO program. Subsequently, APL will perform a new thermal and structural analysis with the modified models to ensure the overall experiment can achieve its science goals and satisfy all NASA-CSBF structural and thermal requirements. APL has sufficient data taken on previous balloon flights to make highly reliable thermal and mechanical predictions. System testing will be conducted at APL's high-bay Balloon Payload Integration facility with a suspension system comparable to the balloon train.

6.2.3 Pointing system

The pointing system will use part of the current SBI system. However, since STO will target objects other than the Sun, a substantial design change will be required to accommodate STO science objectives. The STO pointing specifications are a pointing range of 360° in azimuth and 0 to 54° in elevation, stability $<30''$, pointing knowledge $<15''$, and source acquisition accuracy $<40''$.

The telescope is attached to the gondola on its elevation axis as shown in Figure 18. To point in azimuth the entire gondola will rotate on the vertical axis with angular momentum compensated for by a reaction wheel.

Two operating modes are provided for telescope pointing. Position Mode is used to acquire a source while Inertial Mode is used in inertial tracking and source scanning. In Position Mode STO will use the SBI coarse and intermediate Sun sensors to orient itself towards the target in azimuth with an accuracy of about 0.5°, and it will set the elevation of the telescope according to computed ephemeris with a precision of a 0.17°; see (Bernasconi et al., 2000) and (Bernasconi et al., 2004). The fine acquisition of the target will be done with a star tracker mounted parallel to the telescope optical axis. It will have a field of view of 2°, a position accuracy of $40''$, and a readout rate of 2Hz. APL will select a star tracker based on either BLAST or HERO balloon experiments.

Once fine position knowledge and stability is achieved with the star tracker, the pointing system will transition into Inertial Mode by using position information from two optical Inertial Measurement Units (IMUs), model NL-200 by Northrop Grumman. One IMU will be attached in line with the gondola azimuth rotation axis and used for the gondola fine azimuth control. The second IMU will be attached to the telescope and provide fine elevation pointing error information. Source fine positioning is achieved in both axes by introducing artificial gyro-drift. This method is also used to create line scans, raster patterns and fine source positioning.

The digital control system will be the same as used for FGE and SBI. It uses a Proportional-Integral-Derivative (PID) controller to determine motor drive from sensor position errors. Each pointing mode has 4 control coefficients per axis that can be adjusted in flight for optimum performance.

6.2.4 Power system

The STO power system design will be essentially the same used for SBI (Bernasconi et al., 2004). It consists mainly of three elements: the solar arrays, the charge controller, and the battery stack.

The solar arrays are composed of eight panels each with 65 cells for a total of 520 cells covering a total surface of 8.2 m^2. These model A300 cells from SunPower Corp have 21.5% efficiency. The total power delivered by the arrays is about 1400 W while the estimated total STO power requirement will be only 830 W. This gives us a margin of 570 W. The arrays will be assembled by SunCat Solar of Arizona who previously built the arrays for SBI. The cells will be encased in a transparent laminate on honeycomb substrate that will ensure rigidity and offer good protection to the cells. In 2006 SBI's flight the same type of arrays survived the harsh landing virtually undamaged. To provide the optimum Sun viewing angle while conducting the scientific measurements, APL will attach the STO solar arrays at

at 45° with respect to the front of the gondola and facing to the right (see Figure 18).

The charge controller was originally designed and built for FGE by Meer Instruments of San Diego (CA) who delivered power systems for several NASA LDB payloads including HIGHREGS, BOOMERANG, and ATTIC. It distributes the load across the panels as the power demand changes. It also ensures that the system's battery stacks are maintained at full charge, sunlight permitting, and provides on/off power switching capability from ground commands. It will be the same used for SBI and will require only minor adjustments and updates to accomodate STO's requirements.

The battery stack is composed of four sealed lead-acid ODISSEY PC1700 batteries in an arrangement of two pairs in series connected in parallel. The stack has a capacity of 130 amp-hours with a nominal bus voltage of 24 V. The ODISSEY batteries can operate in vacuum, exhibit great performance characteristics and have an excellent operating temperature range from -40°C to +80°C. We used these batteries for SBI with excellent results.

6.2.5 Command and Control System

Some modifications in the SBI command and control system hardware and software will be required to account for the new STO science control computer and modified attitude control system. Figure 19 gives an overview of the control system.

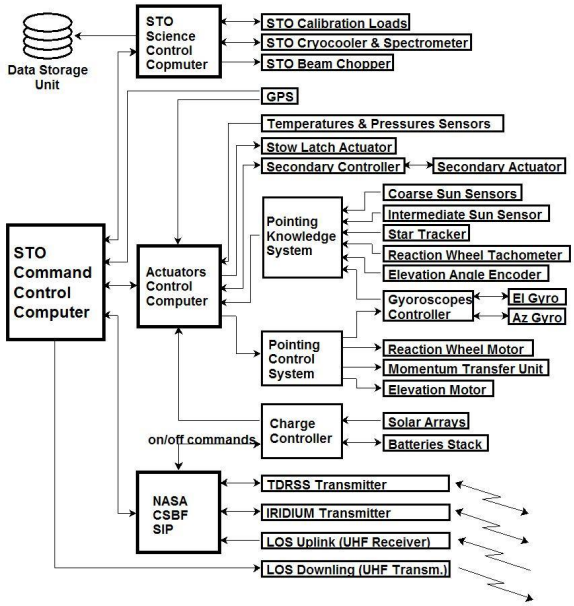

Figure 19: Gondola subsystems block diagram.

There are two main gondola computers on-board: the Command and Control Computer (CCC) and the Actuators Control Computer (ACC). Both computers use a commercial ATX mother board with a Pentium-based CPU, solid state hard drives and Linux as the operating system. They are housed in two pressurized vessels that maintain 1 atmosphere pressure throughout the flight, allowing to use off-the-shelf commercial grade electronic components. The CCC is responsible to schedule all the operations performed by the gondola and handles the communications between the gondola subsystems and the ground. It also communicates to the science computer via an RS232 serial channel. It can operate fully autonomously or execute commands received from the ground. The ACC acts as interface between the CCC computer and all the other gondola subsystems. It gathers all the housekeeping data (temperatures, pressures, voltages, ...) and sends them to the CCC for delivery to the ground. The ACC also handles the attitude control system. It receives position information from all the attitude sensors on-board and computes the control signals for the reaction wheel, momentum dump, and elevation motors to control and stabilize the pointing.

6.2.6 Telecommunications

Similar to the SBI, STO will rely entirely on the NASA-CSBF provided remote link to/from the gondola for the communications between STO and the ground. The communications interface through the SIP is shown in Figure 20. The current communication system works flawlessly and virtually no modifications are needed to adapt it for the STO mission.

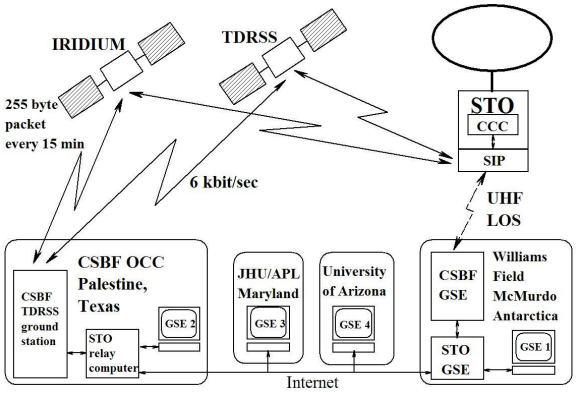

Figure 20: Schematic of the telecommunication system between STO and the ground

The SIP has three available channels to/from the ground. For 24 hours the gondola will be within the

Line-of-Sight (LOS) to the launch station at Williams Field in Antarctica and will use a UHF radio link at a data rate of 38.4 Kb/s. Commands directly from the ground can be used to override normal subsystems automatic operations if necessary. During LOS operations ample amounts of housekeeping data will be available for analysis of both science and gondola performance. Most of the science data will be downlinked through the LOS channel and stored on the ground computers to guarantee a minimum data return from the mission.

After loss of the LOS radio link, communications will be maintained via a 6-Kb/s TDRSS satellite relay and a lower rate IRIDIUM relay (one 255 bytes packet every 15 minutes). The TDRSS and IRIDIUM signals will be received at NASA-CSBF's Operations Control Center (OCC) in Palestine (TX) and relayed to a local STO ground support computer that will redistribute the data packets to other STO ground stations at APL, Univ. of Arizona and to the team in Antarctica. All the STO ground stations will be able to display and store the same telemetry information received at the OCC, and commands can be sent to the gondola computers from any station. Outside of LOS, a reduced data set will be recorded on the ground that will be sufficient to meet the minimum science goals in the case of loss of the payload. The ground support computers will use the software package GSEOS, by GSE Software, Inc., that was previously used for FGE & SBI. This package is widely used at APL to interface with space missions like MESSENGER and New Horizons.

6.3 Data Analysis and Archiving

A primary challenge of On-The-Fly mapping is data management. We therefore plan to adopt a scheme similar to that developed at FCRAO, whereby coadded and regridded data is written as FITS & CLASS files, and headers for each scan are written into a MySQL relational database, which facilitates efficient logging and retrieval of the data. The most demanding storage requirements for 35 sq. degree spectral maps is 10 GB. This volume can be readily handled by embedded computers with nonvolatile FLASH memory. The spatially & spectrally regridded final data product encompasses <500 MB.

While the entire science team will be involved in analysis and interpretation of the data in Spring 2011, near-immediate access of these data products to the greater scientific community will be provided through a web browser interface that interfaces with MySQL and the FITS data cubes. There will be three data product releases in the proposal performance period: (1) a "first flight" data release of the Orion Molecular Cloud in [C II] line emission following the Palestine TX test flight in summer 2010; (2) a preliminary release after the first Antarctic mission in March 2011, and (3) a final release of all data in June 2011. The final release will be fully calibrated and will include all science products.

All science tools, packaged reduction software, data products and catalog products will be made available from the STO survey web page.

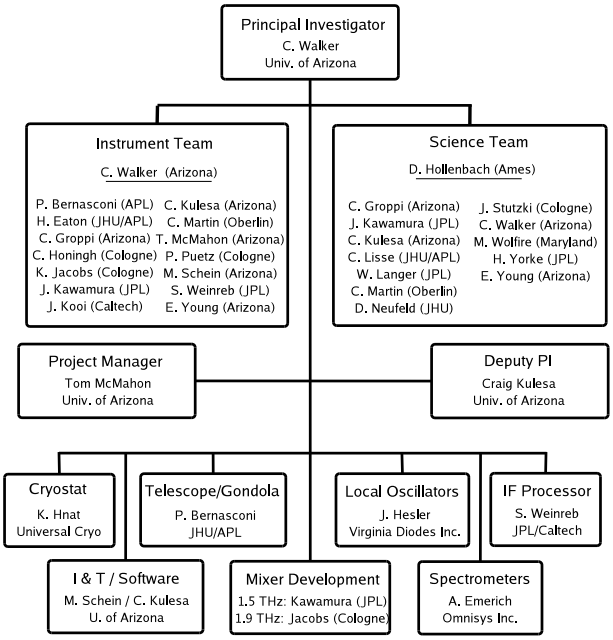

Figure 21: STO Organizational Diagram

7 Management

The STO project brings together an experienced team of researchers from 8 institutions; the University of Arizona, Johns Hopkins Applied Physics Laboratories, NASA Ames Research Center, Jet Propulsion Laboratory, Caltech, Univ. of Maryland, Oberlin College, and the University of Cologne. These organizations and individuals have successfully collaborated on a wide variety of projects in the past and look forward to making STO and the science it will produce a reality.

7.1 Project Management & Organization

The organizational structure of STO, shown in Figure 21 is designed to provide effective control of the project while allowing delegation of authority

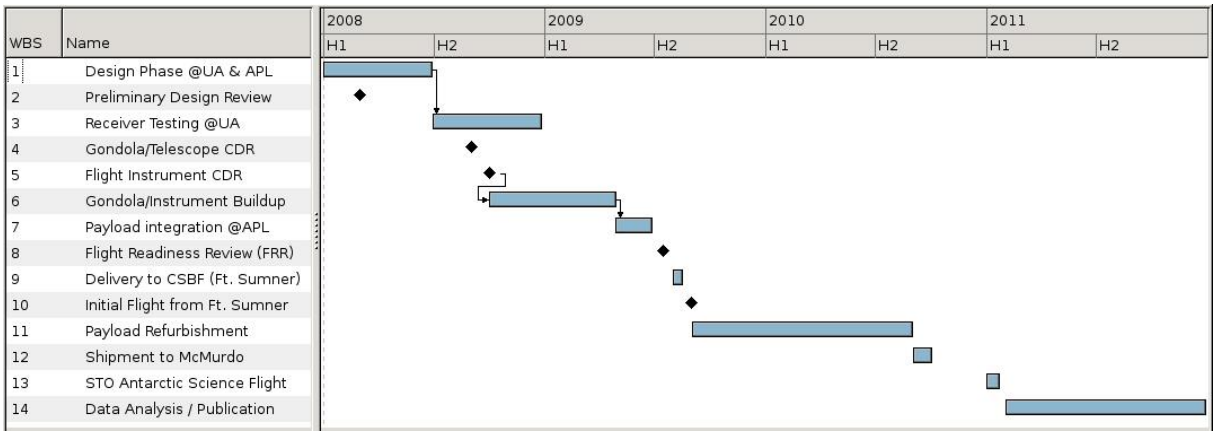

Figure 22: STO Master Schedule

to be made at the proper level within the team. Dr. Walker (PI) is responsible for all aspects of the success and scientific integrity of STO. He will be assisted at the University of Arizona by Dr. Craig Kulesa, who will serve as Deputy PI and Tom McMahon, Project Manager (PM). The STO science team will be led by Dr. David Hollenbach (NASA Ames) who will be STO Project Scientist (PS). The Instrument Team will be led by the PI (Walker). Dr. Bernasconi (APL Institutional PI) will oversee the STO gondola efforts at APL. Dr. Jonathan Kawamura will oversee the 1.46 THz mixer development at JPL. Dr. Karl Jacobs and Dr. Patrick Puetz will oversee the 1.9 THz mixer development at the University of Cologne. Dr. Sander Weinreb will oversee the IF chain development at Caltech. The STO team will make extensive use of electronic communication and management tools including e-mail, secure websites, on-line meetings and video communications to expedite accurate information dissemination. All pertinent management and control information will be posted on a secure STO website maintained by the UA and available to all participants. These tools will be used in daily interactions as well as in weekly team telecons and monthly status briefings to ensure that major issues are visible to and addressed by all affected team members. In addition, face-to-face team meetings will be conducted when appropriate, often in conjunction with program milestones.

7.2 Master Schedule

The master schedule shown in Figure 22 identifies the project's major milestones and development activities. Starting at the Jan. 1 2008 start date, the project would launch into a focused preliminary design phase for the flight hardware and software. This effort culminates in a Preliminary Design Review (PDR) in late March 2008. The scope of the PDR covers the entire flight payload. The project then moves into the critical design phase with Critical Design Reviews for the gondola/telescope and flight instrument held in August and September 2008 respectively. Tests of the [C II] receiver in a lab cryostat are scheduled to commence in December 2008. The flight cryostat construction will be complete in March 2009 with integration and testing of the [C II] receiver in the cryostat in May 2009. Delivery of the flight instrument to JHU/APL for integration into the STO gondola will take place in June 2009. Full system tests will be carried out at APL through July 2009 ending with a Flight Readiness Review (FRR). Following the successful FRR, the STO will be shipped to the CSBF facility for US flight trials in September 2009. After the initial test flight the STO gondola/telescope will be refurbished at APL and the [N II] receiver added to the flight cryostat at the Univ. of Arizona. The final instrument and gondola integration and test will take place at APL in the Spring of 2010. STO will be shipped to Palestine in July-August 2010 where APL will integrate the STO payload with CSBF's balloon control and communication equipment. STO will then be shipped to McMurdo in September 2010. The flight support team members will deploy to McMurdo in Oct. 2010 to prepare STO for the Antarctic flight. The window for flight operations is December 2010 through January 2011. Science data reduction and analysis will start immediately after conclusion of flight operations.

References

Bania, T. M., Lockman, F. J. 1984, "A survey of the latitude structure of galactic H I on small angular scales", ApJS, 54, 513

Bennett, C. L., et al. 1994, "Morphology of the interstellar cooling lines detected by COBE", ApJ, 434, 587

Bernasconi, P. N., Rust, D. M., Eaton, H. A. C., Murphy, G. A. A., 2000, "A Balloon-Borne Telescope for high resolution solar imaging and polarimetry", in "Airborne Telescope Systems", Ed. by R. K. Melugin, and H. P. Röser, SPIE proceedings, 4014, 214

Bernasconi, P. N., Eaton, E. A. C., Foukal, P., Rust, D. M., 2004, "The Solar Bolometric Imager", Adv. Space. Res., 33, 1746

Boreiko, R.T. & Betz, A.L. "The 12C/13C Isotopic Ratio in Photodissociated Gas in M42", ApJL, 467, L113

Dame, T. M., Hartmann, D., Thaddeus, P., 2001, "The Milky Way in Molecular Clouds: A New Complete CO Survey", ApJ, 547, 792

de Avillez, M. A., & Breitschwerdt, D. 2005, "Testing Global ISM Models: A Detailed Comparison of O VI Column Densities with FUSE and Copernicus Data", ApJL, 634, L65

Elmegreen, B. G. 1989, "Molecular Cloud Formation by Gravitational Instabilities in a Clumpy Interstellar Medium", ApJ 347, 561

Engargiola, G., Plambeck, R. L., Rosolowsky, E., & Blitz, L. 2003, "Giant Molecular Clouds in M33. I. BIMA All-Disk Survey", ApJS, 149, 343

Gao, J. R., Hajenius, M., Baselmans, J., Klawijk, P., de Korte, Voronov, B., and Gol'tsman, G., 2004, "NbN Hot Electron Bolometer Mixers with Superior Performance for Space Applications", International Workshop on Low Temperature Electronics, 23-24 June 2004, (invited paper).

Gazol, A., Vázquez-Semadeni, E., & Kim, J. 2005, "The Pressure Distribution in Thermally Bistable Turbulent Flows", ApJ, 630, 911

Grenier, I. A., Casandjian, J.-M., & Terrier, R. 2005, "Unveiling Extensive Clouds of Dark Gas in the Solar Neighborhood", Science, 307, 1292

Heiles, C., & Troland, T. H. 2003, "The Millennium Arecibo 21 Centimeter Absorption-Line Survey. II. Properties of the Warm and Cold Neutral Media", ApJ, 586, 1067

Hennebelle, P., & Pérault, M. 2000, "Dynamical condensation in a magnetized and thermally bistable flow. Application to interstellar cirrus", A&A, 359, 1124

Heyer, M. H., Brunt, C., Snell, R. L., Howe, J. E., Schloerb, F. P., Carpenter, J. M., 1998, "The Five College Radio Astronomy Observatory CO Survey of the Outer Galaxy", ApJS, 115, 241

Heitsch, F., Slyz, A. D., Devriendt, J. E. G., Hartmann, L. W., & Burkert, A., 2006, "The Birth of Molecular Clouds: Formation of Atomic Precursors in Colliding Flows", ApJ, 648, 1052

Hollenbach, D. J., Tielens, A. G. G. M. 1999, "Photodissociation regions in the interstellar medium of galaxies", RvMP, 71, 173

Hu, Q., Williams, B. S., Kumar, S., Callebaut, H., Kohen, S., & Reno, J. L. 2005, Semiconductor Science Technology, 20, 228

Hunter, D. A., Elmegreen, B. G., van Woerden, H. 2001, "Neutral Hydrogen and Star Formation in the Irregular Galaxy NGC 2366", ApJ, 556, 773

Juvela, M., Padoan, P., & Jimenez, R. 2003, "Photoelectric Heating and [C II] Cooling in Translucent Clouds: Results for Cloud Models Based on Simulations of Compressible Magnetohydrodynamic Turbulence" ApJ, 591, 258

Kennicutt, R. C. Jr. 1989, "The star formation law in galactic disks", ApJ, 344, 685

Kim, W.-T. & Ostriker, E.C. 2002, "Formation and Fragmentation of Gaseous Spurs in Spiral Galaxies". ApJ, 570, 132

Kim, W.-T. & Ostriker, E.C. 2007, "Gravitational Runaway and Turbulence Driving in Star-Gas Galactic Disks". ApJ, 646, 213

Kritsuk, A. G., & Norman, M. L. 2002, "Thermal Instability-induced Interstellar Turbulence", ApJL, 569, L127

Kulkarni,S. R., & Heiles, C. 1987, "The atomic component", ASSL Vol. 134: Interstellar Processes, 87

Kwan, J., Valdes, F. 1987, "The spatial and mass distributions of molecular clouds and spiral structure",ApJ,315, 92

Linsky, J. L., and 16 colleagues 2006. What Is the Total Deuterium Abundance in the Local Galactic Disk?. Astrophysical Journal 647, 1106-1124.

Mac Low, M.-M., Balsara, D. S., Kim, J., & de Avillez, M. A. 2005, "The Distribution of Pressures in a Supernova-driven Interstellar Medium. I. Magnetized Medium", ApJ, 626, 864

Martin, C. L., Kennicutt, R. C. Jr 2001, "Star Formation Thresholds in Galactic Disks", ApJ, 555, 301

Martin, C. L., Walsh, W. M., Xiao, K., Lane, A. P., Walker, C. K., and Stark, A. A. 2004, "The AST/RO Survey of the Galactic Center Region. I. The Inner 3 Degrees", ApJS, 150, 239.

McClure-Griffiths, N. M. etal 2005, "The Southern Galactic Plane Survey: H I Observations and Analysis", ApJS, 158, 178

McCray, R., Kafatos, M., 1987, "Supershells and propagating star formation", ApJ, 317, 190

McKee, C. F. 1989, "Photoionization-regulated star formation and the structure of molecular clouds", ApJ, 345, 782

McKee, C. F., Ostriker, J. P. 1977, "A theory of the interstellar medium - Three components regulated by supernova explosions in an inhomogeneous substrate", ApJ, 218, 148

McKee, C. F. Williams, J. P. 1997, "The Luminosity Function of OB Associations in the Galaxy", ApJ, 476, 144

Mueller, E. and Waldman, J., 1994, "Power and Spatial Mode Measurements of Sideband Generated Spatially Filtered, Submillimeter Radiation", MTT, 42, No. 10, 1891.

Mueller, E., Coherent Inc., Private Communication.

Nakagawa, T., Yui, Y. Y., Doi, Y., Oku da, H., Shibai, H., Mochizuki, K., Nishimura, T., & Low, F. J. 1998, "Far-Infrared [C II] Line Survey Observations of the Galactic Plane", ApJS, 115, 259

Neufeld, D. A., Green, J. D., Hollenbach, D. J., Sonnentrucker, P., Melnick, G. J., Bergin, E. A., Snell, R. L., Forrest, W. J., Watson, D. M., Kaufman, M. J. 2006. Spitzer Observations of Hydrogen Deuteride. Astrophysical Journal 647, L33-L36.

Onishi, T. et al., 2005, "New View of Molecular Gas Distribution of the Southern Sky: CO Surveys with NANTEN", in Protostars and Planets V, LPI Contribution No. 1286., p.8301

Ostriker, E. C., & Kim, W.-T. 2004, ASP Conf. Ser. 317: "Milky Way Surveys: The Structure and Evolution of our Galaxy", 317, 248

Parravano, A., Hollenbach, D. J., McKee, C. F. 2003, "Time Dependence of the Ultraviolet Radiation Field in the Local Interstellar Medium" ApJ, 584, 797

Piontek, R. A., & Ostriker, E. C. 2005, "Saturated-State Turbulence and Structure from Thermal and Magnetorotational Instability in the ISM: Three-dimensional Numerical Simulations" ApJ, 629, 849

Schmidt, M. 1959, "The Rate of Star Formation",. ApJ, 129, 243

Steiman-Cameron, T. Y., Wolfire, M. G., & Hollenbach, D. J., "COBE and the Galactic ISM. Geometry of the Spiral Arms" 2007, in preparation.

Taylor, A. R. et al 2002 in "Seeing Through the Dust: The Detection of HI and the Exploration of the ISM in Galaxies", Ed. by A. R. Taylor, T. L. Landecker, and A. G. Willis, (ASP:San Francisco), 68

Taylor, A. R. et al 2003, "The Canadian Galactic Plane Survey", AJ, 125, 3145

Tilanus, R. P. J., Allen, R. J., 1991, "Spiral structure of M51 - Distribution and kinematics of the atomic and ionized hydrogen" A&A, 244, 8

Ulich, B.L., & Haas, R. W., 1976, "Absolute calibration of millimeter-wavelength spectral lines", ApJs 30, 247

Vastel, C., Polehampton, E. T., Baluteau, J.-P., Swinyard, B. M., Caux, E., Cox, P. 2002. Infrared Space Observatory Long Wavelength Spectrometer Observations of C^+ and O^0 Lines in Absorption toward Sagittarius B2. Astrophysical Journal 581, 315-324.

Wiklind, T., Rydbeck, G., Hjalmarson, A., Bergman, P., 1990, "Arm and interarm molecular clouds in M 83", A&A, 232, 11

Williams, J. P., McKee, C. F. 1997, "The Galactic Distribution of OB Associations in Molecular Clouds", ApJ, 476, 166

Wolfire, M. G., McKee., C. F., Hollenbach, D., Tielens, A. G. G. M. 2003, "Neutral Atomic Phases of the Interstellar Medium in the Galaxy", ApJ, 587, 278

Wright, E. L. et al 1991, "Preliminary spectral observations of the Galaxy with a 7 deg beam by the Cosmic Background Explorer (COBE)", ApJ, 381, 200

Zhang, X., Lee, Y., Bolatto, A. D., and Stark, A. A. 2001, "CO (J=4-3) and [C I] Observations of the Carina Molecular Cloud Complex", ApJ, 553, 274.